Ultrasonic power measurement system based on acousto-optic interaction

Liping He,[1] Fulong Zhu,[1,a)] Yanming Chen,[2] Ke Duan,[1] Xinxin Lin,[1] Yongjun Pan,[1] and Jiaquan Tao[1]

[1]*Institute of Microsystems, School of Mechanical Science and Engineering, Huazhong University of Science and Technology, 1037 Luoyu Road, Wuhan, Hubei 430074, People's Republic of China*

[2]*Hubei Institute of Measurement and Testing Technology, East Lake High-Tech Development Zone, Wuhan, Hubei 430223, People's Republic of China*

(Received 29 November 2015; accepted 22 April 2016; published online 12 May 2016)

Ultrasonic waves are widely used, with applications including the medical, military, and chemical fields. However, there are currently no effective methods for ultrasonic power measurement. Previously, ultrasonic power measurement has been reliant on mechanical methods such as hydrophones and radiation force balances. This paper deals with ultrasonic power measurement based on an unconventional method: acousto-optic interaction. Compared with mechanical methods, the optical method has a greater ability to resist interference and also has reduced environmental requirements. Therefore, this paper begins with an experimental determination of the acoustic power in water contained in a glass tank using a set of optical devices. Because the light intensity of the diffraction image generated by acousto-optic interaction contains the required ultrasonic power information, specific software was written to extract the light intensity information from the image through a combination of filtering, binarization, contour extraction, and other image processing operations. The power value can then be obtained rapidly by processing the diffraction image using a computer. The results of this work show that the optical method offers advantages that include accuracy, speed, and a noncontact measurement method. *Published by AIP Publishing.* [http://dx.doi.org/10.1063/1.4948731]

I. INTRODUCTION

Ultrasonic waves are widely used in the medical diagnosis and treatment of the human body.[1–5] However, at the same time, the high intensity output of ultrasonic diagnostic equipment can have negative effects on the villi of the early human embryo, the biochemical metabolism, and the immune function and can thus lead to maldevelopment of the embryo. Long-term research has shown that appropriate levels of ultrasonic power have no ill effects on the human body. It is therefore very important to measure the precise output of an ultrasonic generator.

Two methods are typically used to measure ultrasonic pressure, based on the use of either hydrophones or radiation force balances.[6–8] The conventional method for acoustic pressure measurement using a traditional piezoelectric hydrophone has some drawbacks,[9,10] in that the body of the microphone or hydrophone can affect the acoustic field, and it is difficult to make the body size less than the ultrasonic wavelength when the ultrasonic frequency is too high. Radiation force balances are more attractive measurement instruments than hydrophones because they allow the measurement of absolute ultrasonic power. However, they still have several deficiencies: radiation force balances often require customized design;[11] they have higher measurement uncertainty in practice; and radiation force balances are also unable to provide comprehensive characterization of the acoustic field, including the spatial distribution of energy.

When compared with the conventional methods, acousto-optic interaction[12,13] offers a better option for ultrasonic power measurement, because it is a noncontact method that does not influence the acoustic field. Therefore, in this work, an optical system is used for acoustic power measurement. The optical method is based on acousto-optic interactions in the Raman-Nath regime.[9] When the laser beam intersects with the ultrasound field, it is diffracted and splits into several beams, called the diffracted orders. The light intensities of these diffracted orders contain the required ultrasonic power information, and thus a camera was used to receive the diffraction patterns and transmit them to the computer for subsequent processing. A solid-state laser was chosen as the fundamental element of our measurement setup. The medical ultrasound signal frequency used in abdominal diagnosis and obstetrics applications is usually less than 10 MHz, so the ultrasonic frequency used in this work was set at 950 kHz.

II. SYSTEM MEASUREMENT PRINCIPLE

A. Single-lens optical system

The measurement system is based on the schlieren method, which is an optical imaging technique.[14–19] The principle of the system is illustrated in Fig. 1. The optical lens is an important part of this system. The single-lens optical system can be seen as a linear system. The input into the system is the light signal on plane P1. The lens system transfer function can be determined as long as the transfer function of light in air and the transmittance function of the lens are known, and the output of the single-lens optical system can then be known.

a)Author to whom correspondence should be addressed. Electronic mail: zhufulong@hust.edu.cn. Tel.: +86-27-87557830-801. Fax: 86-27-87557074.

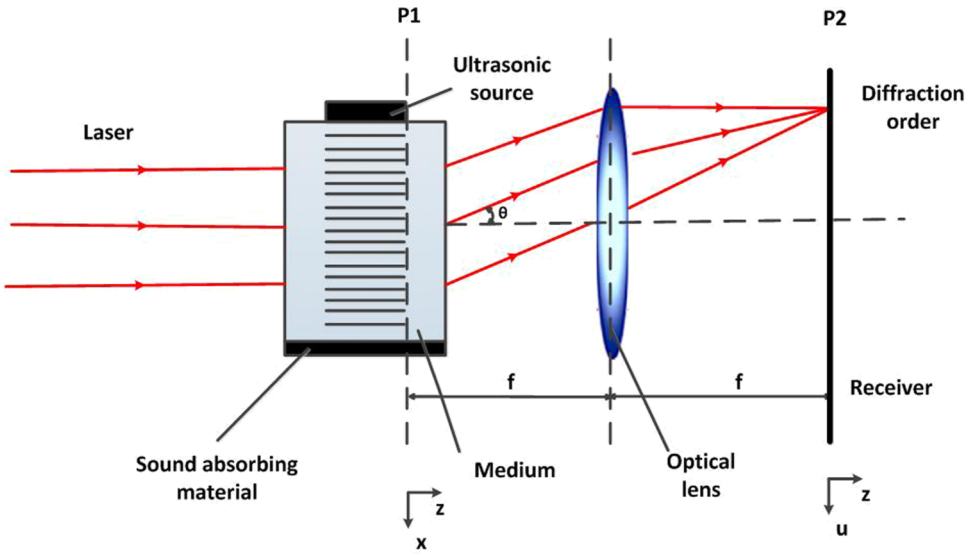

FIG. 1. Principle of the acousto-optical diffraction system.

The Fourier transform of the two-dimensional optics can be used to analyze the optical system.

The optical signal $U(x, y)$, which propagates in free space along the z direction, can be expressed as

$$U(x,y) = U_0(x_0,y_0) * h(x_0,y_0), \tag{1}$$

$$F^T[U(x,y)] = F^T[U_0(x_0,y_0)] * H(f_x,f_y), \tag{2}$$

where $U_0(x_0, y_0)$ is the original optical signal, $F^T[U]$ is the Fourier transform of the function U, and the transfer function $h(x, y)$ and the response function $H(f_x, f_y)$ are described as

$$h(x,y) = \frac{e^{jkz}}{j\lambda z} e^{\frac{jk}{2z}(x^2+y^2)}, \tag{3}$$

$$H(f_x,f_y) = \frac{e^{jkz}}{j\lambda z} e^{-j\pi\lambda z(f_x^2+f_y^2)}. \tag{4}$$

$k = 2\pi/\lambda$ is the laser wave number in a vacuum, λ is the laser wavelength, and f_x and f_y are the spatial frequencies, which can be defined as

$$f_x = \frac{x}{\lambda z}, f_y = \frac{y}{\lambda z}. \tag{5}$$

If that the center thickness of the lens is Δ_0 and its focal length is f, then its transmittance is t_I

$$t_I(x,y) = \frac{U_I(x,y)}{U(x,y)} = \exp(jkn\Delta_0)\exp(-\frac{jk}{2f}(x^2+y^2)). \tag{6}$$

n is the refractive index of the lens material, $U(x, y)$ is the input light wave on plane P1, and $U_I(x,y)$ is the output light wave on plane P2. Because $\exp(jkn\Delta_0)$ is constant, it can be ignored and the simplified transmittance is thus expressed as follows:

$$t_I(x,y) = \exp(-\frac{jk}{2f}(x^2+y^2)). \tag{7}$$

This demonstrates that the lens in the optical system plays a role in the phase modulation behavior.

In the lens system shown in Fig. 1, the input plane is the front focal plane P1, and the output plane is the rear focal plane P2, and based on Equations (1) and (7), it can be shown that

$$\begin{aligned} U_f(u,v) &= h(u,v) * U_I(x,y) \\ &= \frac{e^{jkf}}{j\lambda f}\iint_{s_0} t_I(x,y)\,U(x,y)\,e^{\frac{jk}{2z}[(x-u)^2+(y-v)^2]}dxdy \\ &= \frac{e^{jkf}e^{\frac{jk}{2z}(u^2+v^2)}}{j\lambda f}F^T[U(x,y)]_{f_x=\frac{u}{\lambda f},f_y=\frac{v}{\lambda f}} \\ &= \frac{e^{j2kf}}{\lambda^2 f^2}F^T[U_0(x_0,y_0)]_{f_x=\frac{u}{\lambda f},f_y=\frac{v}{\lambda f}}. \end{aligned} \tag{8}$$

This means that the optical signals from the front focal plane and the back focal plane are strictly Fourier transform signals.

B. Acousto-optic diffraction

When an ultrasonic wave propagates through a medium, it will generate periodic changes in the density of the medium. Then, a corresponding periodic change also occurs in the refractive index at each point in the medium. The periodic distribution of the refractive index in the medium is equivalent to a "phase grating" and can be called an ultrasonic grating. When a light beam propagates through the medium, the grating will generate diffraction phenomena. The "phase grating" formed by the ultrasonic wave is a type of real-time grating that can be erased, and the grating constant can be controlled by the frequency of the ultrasonic wave. It is therefore convenient to use the ultrasonic waves to control the intensity and direction of the light beam, while the light beam will not produce any interference in the acoustic field.

When a light beam propagates through the acoustic field in a medium, then either Raman-Nath or Bragg diffraction takes place. The criterion for the Raman-Nath diffraction regime is defined by the Klein–Cook parameter Q. When $Q < 1$,

Raman-Nath diffraction occurs,[20]

$$Q = \frac{2\pi\lambda L}{n_0{\lambda_a}^2}. \tag{9}$$

In Equation (9), L is the length of the interaction volume, λ is the laser light wavelength in a vacuum, λ_a is the acoustic wavelength in the interaction medium, and n_0 is the refractive index in the medium without application of ultrasound. The upper frequency limit of the Raman-Nath regime in a solution could reach up to 30 MHz,[21] and if the acousto-optic device material is changed to a crystalline material, then the upper frequency limit of the Raman-Nath regime will increase.

When a planar ultrasonic wave with acoustic pressure $p = p_a \sin(\omega_a t - k_a x)$ propagates through a medium along the x direction, it modulates the phase of the planar light, $A\exp(\omega t - kz)$, which propagates along the z direction. The light signal in the front focal plane P1 can then be described as

$$U_0(x,t) = Ae^{j\omega t}\exp\left[jk\frac{\alpha_p}{\rho_0 c_0^2}LP_a\sin(\omega_a t - k_a x)\right]. \tag{10}$$

In Equation (10), A is the amplitude of the light wave, ω and ω_a are the circular frequencies of the light and ultrasonic waves, respectively, k and k_a are the wave numbers of the light and ultrasonic waves, respectively, ρ_0 is the density of the medium, c_0 is the speed of sound in the medium, L is the length of the acousto-optic interaction, and α_p is the adiabatic piezo-optic coefficient calculated from the refractive index of the medium. If the laser light wavelength is 632.8 nm, then the adiabatic piezo-optic coefficient of water is 0.323, and from Equation (8), the light signals in the rear focal plane P2 are

$$\begin{aligned} U_f(u,t) &= A'e^{j\omega t}F^T\left[e^{jk\frac{\alpha_p}{\rho_0 c_0^2}LP_a\sin(\omega_a t - k_a x)}\right] \\ &= A'e^{j\omega t}F^T\left[\sum_{m=-\infty}^{\infty}J_m\left(k\frac{\alpha_p}{\rho_0 c_0^2}LP_a\right)e^{-jmk_\alpha x}e^{jm\omega_\alpha t}\right] \\ &= A'e^{j\omega t}\sum_{m=-\infty}^{\infty}e^{jm\omega_\alpha t}J_n\left(k\frac{\alpha_p}{\rho_0 c_0^2}LP_a\right)\delta\left(\frac{m}{\lambda_a} - \frac{u}{\lambda f_2}\right). \end{aligned} \tag{11}$$

In the above expression

$$e^{jz\sin\theta} = \sum_{m=-\infty}^{\infty}J_m(v)\,e^{jm\theta}. \tag{12}$$

$J_m(v)$ is a Bessel function of the first kind, and Equation (11) shows that there will be a series of discrete diffraction light spots along the u direction in the transform plane, where all levels of the diffraction intensity are given by

$$I_m = A'^2 J_m^2(v), \tag{13}$$

$$v = k\frac{\alpha_p}{\rho_0 c_0^2}LP_a. \tag{14}$$

Thus, by measuring all levels of the diffraction intensity, the ultrasonic wave pressure can be obtained. The Bessel function of the first kind meets the following rules:

$${J_m}^2(v) = {J_{-m}}^2(v), \tag{15}$$

$${J_0}^2(v) + 2\sum {J_m}^2(v) = 1. \tag{16}$$

Assuming that the medium does not assimilate the light, the sum of the Raman-Nath diffraction intensities at the various levels is equal to the incident light intensity, i.e.,

$$\frac{I_m}{I} = {J_m}^2(v), \tag{17}$$

where I is the value of the light intensity with no ultrasonic waves. Therefore, it is only necessary to measure the relative change in the diffraction intensity at the different levels. We can thus obtain the v value by consulting the Bessel function table and calculate the ultrasonic pressure or power as follows:

$$\mathrm{P} = \frac{\rho_0 {c_0}^3 \lambda^2 v^2}{32\pi(n_0 - 1)^2}e^{2ah}, \tag{18}$$

where a is the sound attenuation coefficient in the medium, and h is the distance from the ultrasonic transducer surface to the light beam.

C. Diffraction pattern processing

In this work, an area array charge-coupled device (CCD) was used as the light intensity sensor. CCD sensors offer many advantages, including high sensitivity, a wide spectral response, a large dynamic range, small pixel size, high geometric accuracy, good vibration resistance, and low cost. CCD sensors are therefore a good choice as a means of obtaining image information, and a corresponding method to perform

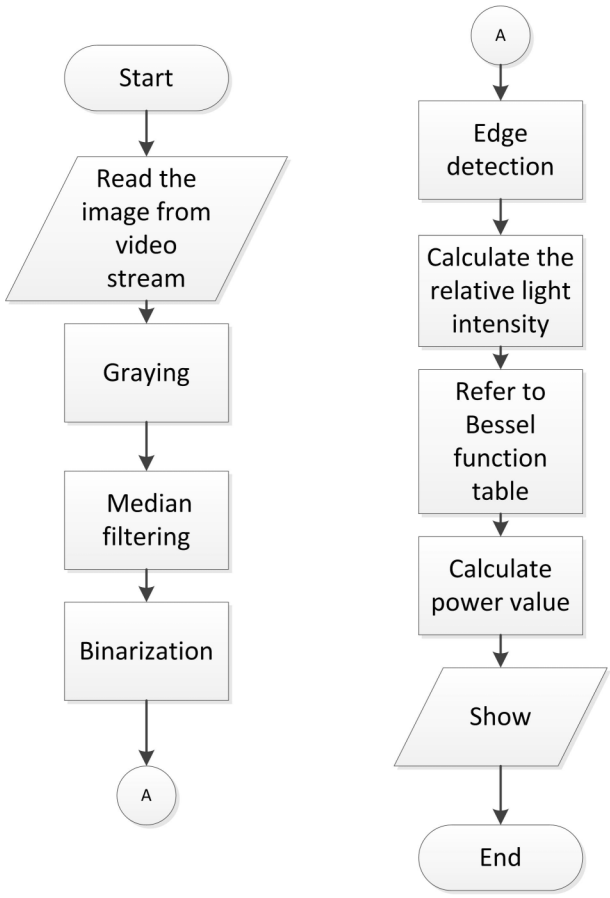

FIG. 2. Software processing flow chart.

image analysis is also required. Figure 2 shows a diagram of the image processing flow.

In image processing, to reduce the amount of data to be processed, it is a common practice to convert the three-channel image into a gray image. Initially, therefore, the original image should be converted into a grayscale image.

The gray image must be filtered before use, and in this work, a median filter is selected to deal with the gray image. A median filter is a typical type of low pass filter; its purpose is to protect the image edge while removing the noise, and it is the most effective method for filtering of the pulse interference. The median filter can easily remove isolated point and line noise but is powerless against Gaussian noise. The results of the use of a median filter are shown in Fig. 3(b).

After filtering, image binarization is performed. The most important aspect of binarization is calculation of the image threshold, and the Otsu method[22] is a good choice for this task. Figure 3(c) shows the results of binarization, and the edge of the image can be obtained as shown in Fig. 3(d).

The purpose of image processing is to obtain the value of $J_m{}^2(v)$. From Equation (17), it is necessary to determine the overall light intensity value and the intensity values at various diffraction levels. Because the gray value in a monochrome image reflects the intensity of the light, this means that the sum of the gray values indicates the light intensity of a diffraction level or the overall light intensity. Using image-processing algorithms, it can be possible to very rapidly distinguish between the edges of the different levels and sum up the corresponding gray value.

III. EXPERIMENTAL RESULTS AND DISCUSSION

As shown in Fig. 4, the complete measurement system consists of eleven parts. The fine parallel beam that is

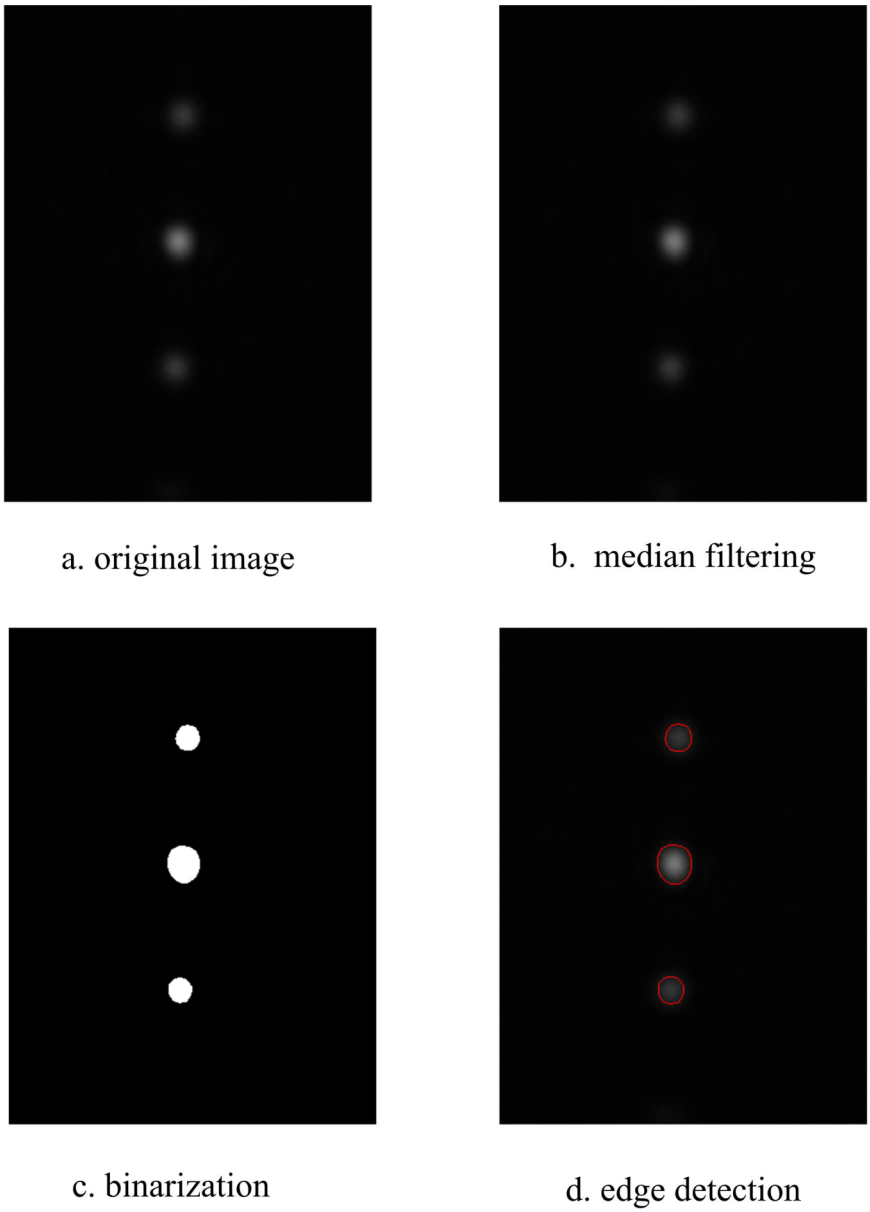

FIG. 3. Image processing stages.

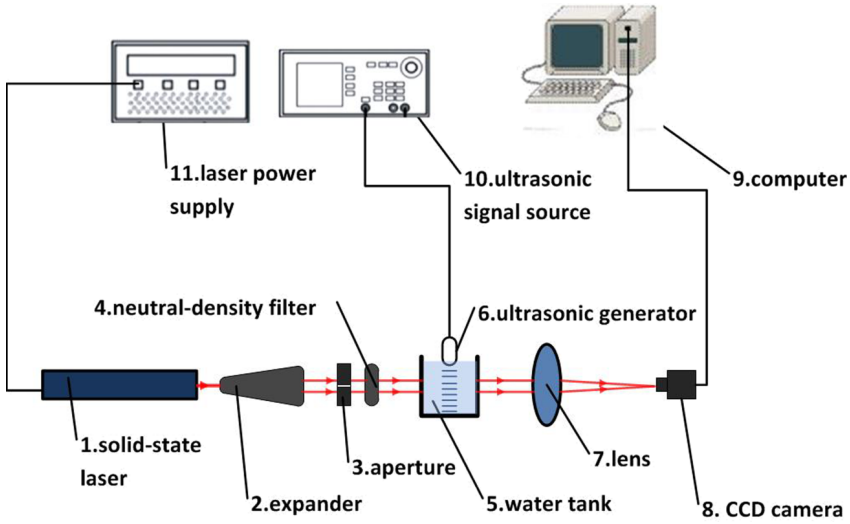

FIG. 4. Structural diagram of the measurement system.

generated by the solid-state laser tube (1) is magnified by the expander (2), and the parallel beam changes into a narrow planar light beam in the aperture (3). The neutral-density filter (4) is used to weaken the light intensity so that the CCD camera (8) will not be overloaded. The light ray then interacts with the ultrasonic waves in the water tank (5), where (6) is the ultrasonic generator. The lens (7) is used to focus the image of the acousto-optic diffraction on the CCD camera (8) and the image is then passed to the computer (9), where ultimately software is used to calculate the ultrasonic power value. (10) is the ultrasonic signal source, and (11) is the laser power supply. The water and the glass tank can be replaced by another crystal in practical measurements. The practical prototype of the proposed measurement system is shown in Fig. 5.

At the beginning of the measurement process, it is necessary to adjust the solid-state laser, the expander, the lens and the CCD camera to meet the coaxial location requirement so that the image is shown at the center of the CCD camera. During this process, the ultrasonic generator and the CCD camera are both turned off.

To evaluate the feasibility of the proposed measurement system, a high-power ultrasonic generator was used as the ultrasonic source to enable the system to generate obvious diffraction patterns. Then, the rules of the changes in light intensity were analyzed, and the results were found to be consistent with a Bessel function of the first kind. These results proved that the measurement system is both correct and feasible. The patterns of the different diffraction orders are shown in Fig. 6.

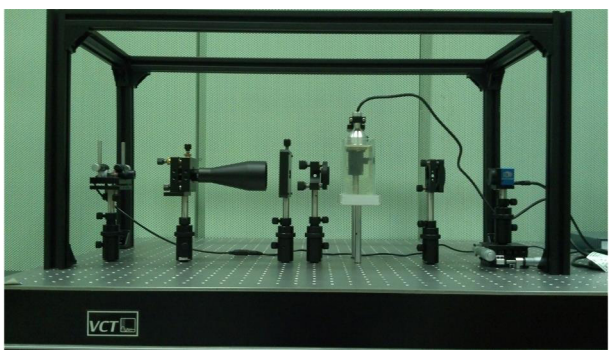

FIG. 5. Practical prototype of proposed measurement system.

The parallel light was focused on a spot without ultrasonic wave loading, as shown in Fig. 6(a). To make this phenomenon obvious, the gray value of the spot has reached 255. Therefore, the gray value cannot reflect the real light intensity information. When the power of the ultrasonic generator increased, part of the light intensity was diverted from the zero level to the first level, as shown in Fig. 6(b). When the power of the ultrasonic wave increased sequentially, the light intensity of the first level gradually strengthened, as shown in Fig. 6(c). When the ultrasonic power increased to a specific threshold value, the second level showed and the total light intensity was split into all the diffraction orders, so the brightness of the diffraction pattern was subsequently very weak, as shown in Fig. 6(d). Figure 7 shows the variation of the light intensity from theory. The value $J_m^2(v)$ indicates the relative light intensity and the variable v is correlated positively with the ultrasonic power, as shown in Equation (14). It can thus be concluded that the actual change in the diffraction light intensity is consistent with the theory, which thus proves the correctness of the proposed ultrasonic measurement system.

After the correctness of the measurement system was verified, a low-power ultrasonic generator was then measured. To ensure that the gray value of the image correctly reflects the light intensity information, the maximum gray value cannot exceed 255. Before the measurement is performed, all parameters apart from v in Equation (18) should be set to the appropriate values. Table I shows the values of some of the parameters used in this experiment.

When the program begins the measurement process, it can determine the edges of the light spots and draw them on the screen, as shown in Fig. 8(a). As the power of the ultrasonic wave increases, the diffraction level also increases from zero to one.

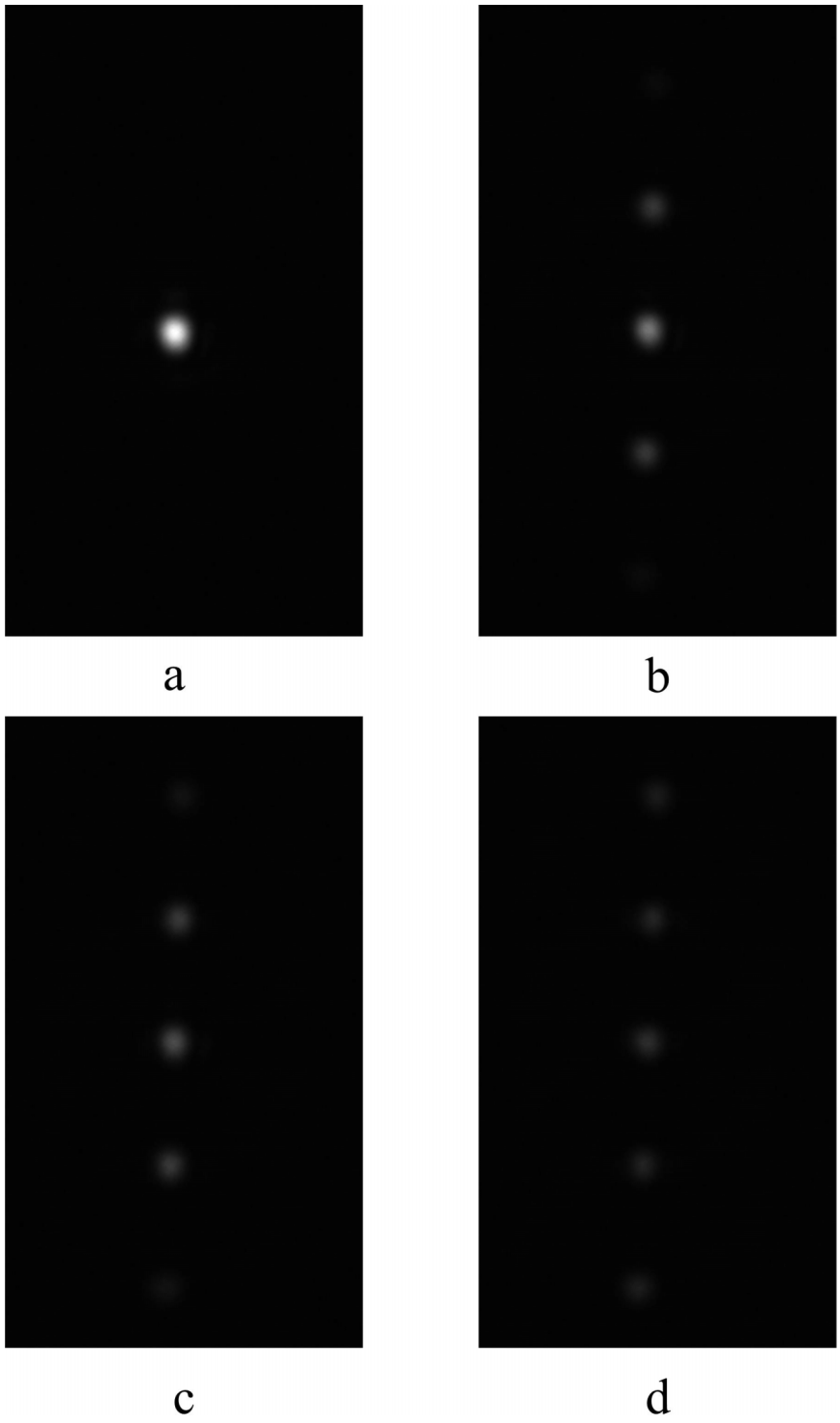

FIG. 6. Diffraction patterns of the different levels, where (a) is the zero level image, (b) and (c) are the images that have the first level spots, and (d) is the image that has the second level spots.

Using the image processing software, the value of $J_m^2(v)$ can be determined, but our goal is to obtain the variable v and substitute it into Equation (18) to calculate the ultrasonic power. Because the function $J_m^2(v)$ shown in Fig. 7 is not invertible, it is likely that several v values can be determined from a specific $J_m^2(v)$. To solve this problem, the software first creates a matrix such that its rows and columns correspond to v and $J_m^2(v)$, respectively. The software then searches for the values of v in this matrix for every possible $J_m^2(v)$. Every $J_m^2(v)$ value will then be searched for one or more v values that can be placed in a specific array; there must be two closest v values in two arbitrary arrays and the number of all closest v values is equal to the number of diffraction levels. The average value v_0 calculated from those v values is the final step, and by substituting v_0 and the other necessary parameters into Equation (18), the power of the ultrasonic wave can be

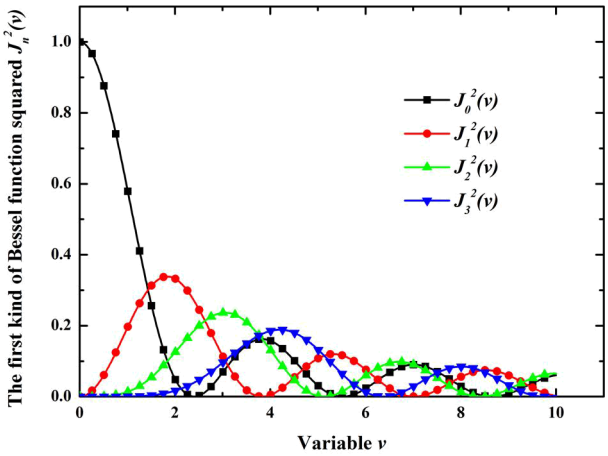

FIG. 7. Bessel function of the first kind squared.

TABLE I. Experimental parameter values.

Parameters	Values	Units
ρ_0	1000	kg/m^3
c_0	1450	m/s
λ	632.8×10^{-9}	m
n_0	1.33	
a	0.021	dB/m
h	0.02	m

determined. The powers of the images from Figs. 8(a)–8(d) are (a) 0.022 W, (b) 0.077 W, (c) 0.115 W, and (d) 0.139 W. Because the maximum gray value does not exceed 255, the intensity of the zero level will be moved to the first level when the ultrasonic power increases, and the entire image will appear to be very dark.

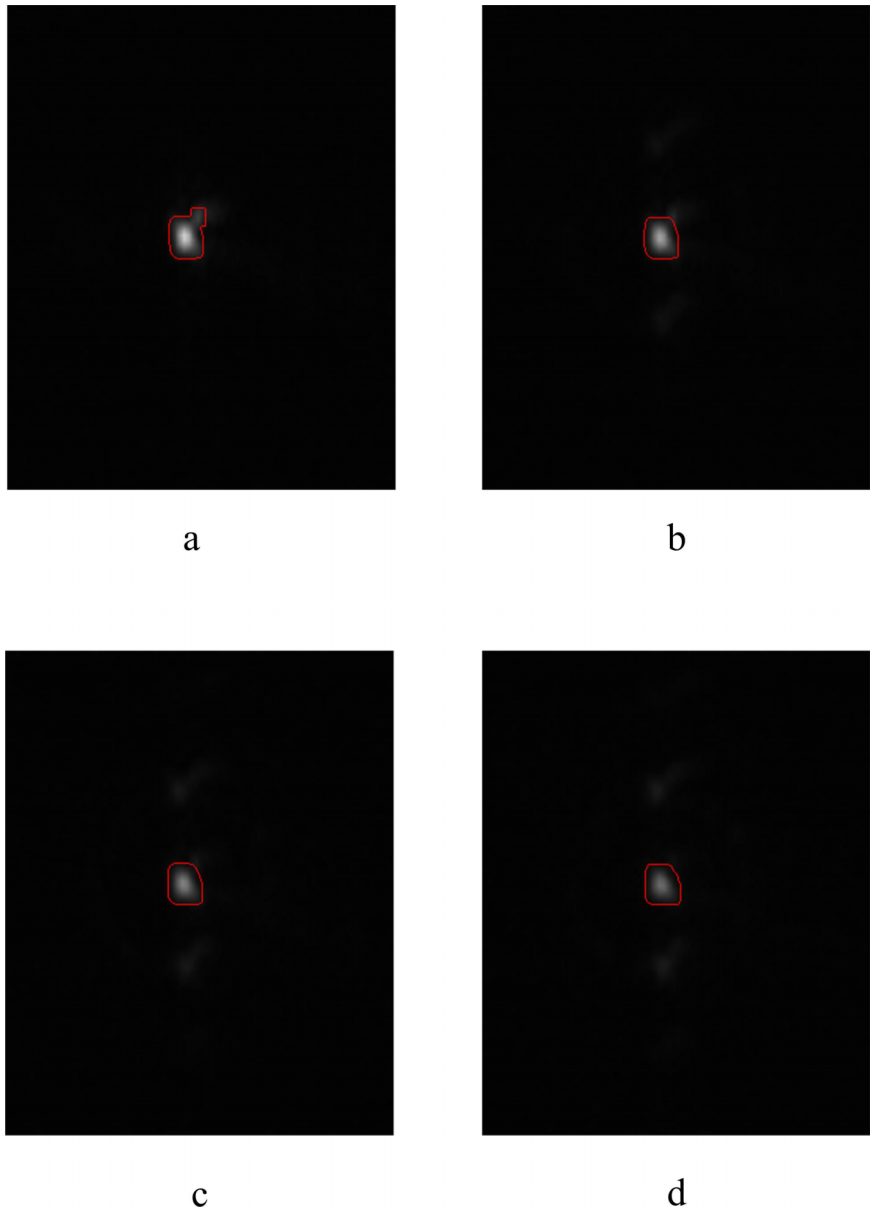

FIG. 8. Diffraction patterns for various powers, where the powers in the images are (a) 0.022 W, (b) 0.077 W, (c) 0.115 W, and (d) 0.139 W.

IV. CONCLUSIONS

The results show that the acousto-optic method proposed here for acoustic power measurement in a water medium is superior to the conventional methods that were described earlier. One obvious advantage is that the acousto-optic method does not affect the acoustic field. Also, the measurement system has a wide frequency response range, as long as the Klein–Cook parameter $Q \ll 1$. In addition, the measurement system can be used continuously when both the frequency and the power are changing. When compared with the radiation force balance method, the measurement system has lower measurement uncertainty and also has a stronger anti-jamming capability. The measurement system described in this work is highly suitable for both industrial and biomedical ultrasonic applications, because it has lower environmental demands than the other established methods. Of course, the measurement system has some limitations, such as the fact that the system cannot describe the spatial distribution of the acoustic field. In addition, the medium and the container walls must be transparent.

ACKNOWLEDGMENTS

This work is supported by the 973 Project (Grant No. 2015CB057203) and the Fundamental Research Funds for the Central Universities (HUST: Grant No. 2013TS023). The technical assistance and suggestions provided by Dr. Dong Lin of Purdue University are greatly appreciated by the authors.

[1]J. Lindner, F. J. Villanueva, K. Wei, J. Sklenar, and S. Kaul, Am. Heart J. **139**(2), 231 (2000).
[2]B. Tutschek, P. Robertson, S. Wyatt, C. Sahn, H. Ling, and D. Sahn, Am. J.Obstet. Gynecol. **195**(6), S77 (2006).
[3]A. Caronti, G. Caliano, R. Carotenuto, A. Savoia, M. Pappalardo, E. Cianci, and V. Foglietti, Microelectron. J. **37**(8), 770 (2006).
[4]A. Dan, S. Beilin-Nissan, Z. Friedman, and V. Behar, Ultrasonics **44**(2), 166 (2006).
[5]S. M. Howard and C. I. Zanelli, paper presented at the IEEE Ultrasonics Symposium, 2007.
[6]T. Kikuchi, S. Sato, and M. Yoshioka, Jpn. J. Appl. Phys., Part 1 **41**(5B), 3279 (2002).
[7]K. Beissner, J. Acoust. Soc. Am. **124**(4), 1941 (2008).
[8]G. R. Harris, Ultrasound Med. Biol. **11**(6), 803 (1985).
[9]Z. Šlegrová and R. Bálek, Ultrasonics **43**(5), 315 (2005).
[10]Z. Bartáková and R. Bálek, Ultrasonics **44**(Suppl. 1), e1567 (2006).
[11]Y. Wu, P. M. Shankar, P. A. Lewin, and D. P. Koller, IEEE Trans.Ultrason., Ferroelectrics Freq. Control **41**(2), 166 (1994).
[12]M. Almqvist, A. Holm, H. W. Persson, and K. Lindström, Ultrasonics **37**(8), 565 (2000).
[13]O. B. Matar, L. Pizarro, D. Certon, J. P. Remenieras, and F. Patat, Ultrasonics **38**(1-8), 787 (2000).
[14]P. A. Chinnery, V. F. Humphrey, and C. Beckett, J. Acoust. Soc. Am. **101**(1), 250 (1997).
[15]C. Unverzagt, S. Olfert, and B. Henning, Phys. Procedia **3**(1), 935 (2010).
[16]N. Kudo, Y. Sanbonmatsu, and K. Shimizu, paper presented at the IEEE Ultrasonics Symposium (IUS), 2010.
[17]G. Zhu, X. F. Zhu, and L. Liu, Acta Acust. **18**, 304 (1999).
[18]G. Z. Zhu, L. Liu, and D. Y. Fu, Chin. Phys. Lett. **16**(11), 819 (2008).
[19]G. Zhu, K. Lu, D. Fu, and Y. Yang, Meas. Sci. Technol. **13**(4), 483 (2002).
[20]M. G. Moharam and L. Young, Appl. Opt. **17**(11), 1757 (1978).
[21]K. Ikeda, Proc. IEEE Ultrason. Symp. **3**, 1860 (2004).
[22]N. Otsu, IEEE Trans. Systems **9**, 62 (1979).